# Advective and diffusive contributions to reactive gas transport during pyrite oxidation in the unsaturated zone

Binning, P. J.; POSTMA, D; Russell, T. F.; Wesselingh, J. A.; Boulin, P. F.

*Published in:*
Water Resources Research

*DOI:*
10.1029/2005WR004474

# Advective and diffusive contributions to reactive gas transport during pyrite oxidation in the unsaturated zone

P. J. Binning,[1] D. Postma,[1] T. F. Russell,[2] J. A. Wesselingh,[3] and P. F. Boulin[1]

Received 29 July 2005; revised 23 August 2006; accepted 21 September 2006; published 14 February 2007.

[1] Pyrite oxidation in unsaturated mine waste rock dumps and soils is limited by the supply of oxygen from the atmosphere. In models, oxygen transport through the subsurface is often assumed to be driven by diffusion. However, oxygen comprises 23.2% by mass of dry air, and when oxygen is consumed at depth in the unsaturated zone, a pressure gradient is created between the reactive zone and the ground surface, causing a substantial advective air flow into the subsurface. To determine the balance between advective and diffusive transport, a one-dimensional multicomponent unsaturated zone gas transport model is developed. Both advection-diffusion and Maxwell-Stefan model formulations are presented. A steady state analytical solution is derived that provides insight into solution behavior and which can be used to test numerical models. A numerical solution is obtained for both the steady and transient cases. At steady state, advection comprises approximately 23% of the total oxygen flux, with the contribution of advection being almost entirely determined by the composition of the atmosphere. Other parameters, such as the permeability, have a negligible effect on the proportion of advective flows at steady state. However, greater pressure gradients are found in low-permeability soils. In transient cases, advective fluxes depend on the initial conditions and can be far greater than diffusive fluxes. In contrast to steady state conditions the transient case is sensitive to other model parameters; for example, the time to approach steady state depends exponentially on the distance between the soil surface and the subsurface reactive zone.

**Citation:** Binning, P. J., D. Postma, T. F. Russell, J. A. Wesselingh, and P. F. Boulin (2007), Advective and diffusive contributions to reactive gas transport during pyrite oxidation in the unsaturated zone, *Water Resour. Res.*, *43*, W02414, doi:10.1029/2005WR004474.

## 1. Introduction

[2] Pyrite oxidation is an important geochemical reaction. It can generate extreme conditions such as those observed in acidification of mine waste [*Nordstrom et al.*, 2000], and can also lead to less concentrated, but still important impacts due to the appearance of contaminants in groundwater systems that are modified by pumping [*Larsen and Postma*, 1997].

[3] The oxidation of pyrite in the unsaturated zone is often limited by the availability of oxygen and so the transport of oxygen from the atmosphere into the soil becomes rate determining [*Davis and Ritchie*, 1986; *Wisotzky*, 1994; *Elberling and Nicholson*, 1996]. To predict pyrite oxidation rates, the transport of oxygen in the unsaturated zone is therefore modeled. However, many of these models consider only diffusive processes [*Elberling and Nicholson*, 1996]. New experimental research is emerging which shows that substantial gas volume changes often occur as a result of pyrite oxidation. The possibility that such volume changes drive significant advective fluxes is investigated in this paper.

[4] Many gas transport models are currently available for analyzing the pyrite oxidation problem, and some include advective fluxes driven by compositional and density changes. However, few focus on determining the advective flux caused by gas volume changes during pyrite oxidation. Here an idealized problem is considered with this aim. A steady state analytical solution is developed that provides new insight into advective driven flow processes and which can be used to benchmark numerical models. Numerical solutions are then obtained to examine more general and transient cases.

[5] *Davis and Ritchie* [1986] were among the first to recognize the importance of oxygen transport for subsurface reactions and developed a diffusive model to determine rates of pyrite oxidation in mine waste rock dumps. Models based on a diffusive oxygen transport assumption are still predominant, for example those of *Bronswijk et al.* [1993], *Wunderly et al.* [1996], *Gerke et al.* [2001] and *Molson et al.* [2005].

[6] Only a few authors have considered the implications of compositional changes on pressure and gas advection. *Cathles and Apps* [1975] set up a combined heat and

[1]Institute of Environment and Resources, Technical University of Denmark, Lyngby, Denmark.
[2]Division of Mathematical Sciences, National Science Foundation, Arlington, Virginia, USA.
[3]Department of Chemical Engineering, University of Groningen, Groningen, Netherlands.


0043-1397/07/2005WR004474

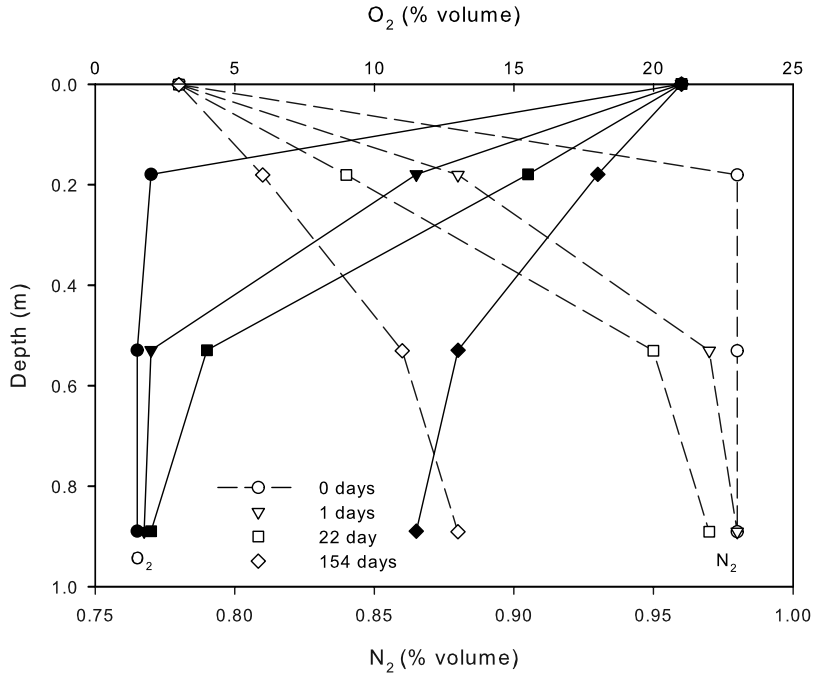


**Figure 1.** Experiment of *Wisotzky* [1994], showing transport of oxygen into a column initially filled with nitrogen and pyrite. Shown are measured oxygen and nitrogen profiles as a function of time.

oxygen transport model where transport is determined by heat and density induced convection. Gas advection was calculated from a pressure decrease due to concentration and temperature changes. This paper derives a different form for the advection term to that obtained by *Cathles and Apps* [1975]. For example, *Cathles and Apps* [1975] suggested that the advective flux is proportional to the material permeability. In contrast, the advective flux is shown in this paper to be independent of permeability at steady state and only slightly dependent in transient cases. *Thorstenson and Pollock* [1989] were the first to develop a Maxwell-Stefan model of the process and showed that 18.5% of the gas flux at the surface could be advective. This paper extends that work by developing some new analytical and numerical solutions and also by considering temporal changes to the advective fluxes. At the same time as the work of *Thorstenson and Pollock* [1989], *Sleep and Sykes* [1989] developed a model that included density driven gas phase advection and demonstrated the importance of that advective process for NAPL transport. Other important early work includes that of *Harries and Ritchie* [1985] (and a subsequent paper by *Pantelis and Ritchie* [1991]) who considered gas volume changes, but only in response to reaction driven temperature changes. These papers laid the foundation for models of gas transport in chemically active groundwater systems.

[7] Research activity on gas flow in porous media has continued since these landmark papers, but there has been little attention paid to gas advection due to reactive processes. *Simunek and Suarez* [1993] formulated an advection diffusion model of $CO_2$ transport, but then assumed that the advective component is small and did not consider it further. *Kuo and Ritchie* [1999] consider the impact of compositional changes to gas advection. However, when calculating advective flows, only compositional changes to density under constant pressure are considered and an upward flux due to buoyancy is predicted. In contrast this paper considers pressure changes and predicts a downward advective flux. *Xu et al.* [2000] and *Xu and Pruess* [2001] constructed a multicomponent geochemical transport model of pyrite oxidation, but do not consider changes of density due to gas compositional changes. *Pantelis et. al* [2002] presented a comprehensive gas transport model, but do not focus on the importance of compositional changes on gas density as is done here. *Costanza-Robinson and Brusseau* [2002] also set up a more general gas flow model, but did not consider reaction induced volume changes. *Mayer et al.* [2002] present a multicomponent geochemical transport model of species transport in mine tailings, but do not consider advective gas transport. *De Visscher and Van Cleemput* [2003] examine four component reactive gas flow in a landfill. They employ a Maxwell-Stefan formulation that does account for gas volume changes, but do not focus on that issue in their paper. Finally, *Kim and Benson* [2004] do consider both advection and diffusion in landfill liners, but do not consider the impact of oxygen consumption on gas pressure and consider only single component gas transport. They conclude that oxygen transport is 99% diffusion dominated, a conclusion that is not supported by this work.

[8] Recent experimental work suggests that more consideration should be given to gas advection in reactive flow problems. For example, *Wisotzky* [1994] and *van Berk and Wisotzky* [1995] measured gas composition and pyrite content in a waste rock dump as a function of depth and time and concluded that advection was necessary to explain the observed gas composition. The conclusion follows from the observation that an advective flux is necessary to explain the nitrogen enrichment with depth that is observed in column studies and at field sites [*van Berk and Wisotzky*, 1995]. One set of results from the experiments of *Wisotzky* [1994] on the time evolution of gas composition in a column initially filled with nitrogen and pyrite is shown in Figure 1.

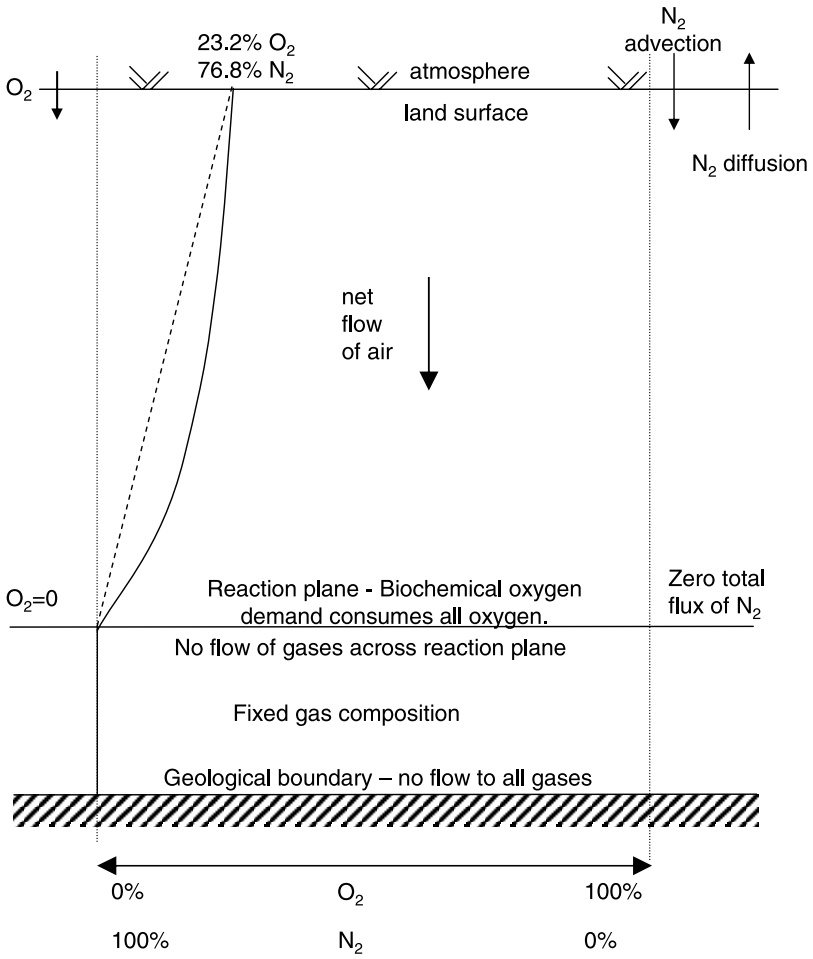


**Figure 2.** Schematic of problem. The dotted profile shows the diffusive gas composition profile at steady state assumed by most authors. The solid line shows an exaggerated representation of the profile when gas advection is considered. From *Binning et al.* [2004], copyright (2004), with permission from Elsevier.

While the results in Figure 1 do not illustrate the nitrogen enrichment process, they are a nice demonstration of gas compositional changes due to pyrite oxidation. In a more recent paper, *Amos et al.* [2005] considered experimental data and showed that advective fluxes could be significant at a crude oil spill site.

[9] To investigate gas volume changes under controlled conditions, *Andersen et al.* [2001] conducted batch experiments which indicated that gaseous volume losses of 20% in the reaction of pyrite with air and water could occur. The volume loss can be explained by examining the reaction

$$FeS_2 + \frac{15}{4}O_2 + \frac{7}{2}H_2O \rightarrow Fe(OH)_3 + 2SO_4^{2-} + 4H^+ \quad (1)$$

In the reaction gaseous oxygen is consumed, leading to a loss of gaseous volume. If calcite is present, then $CO_2$ is produced partially offsetting the loss of volume due to oxygen removal and leading to total volume losses of 10%.

[10] To analyze the relative importance of advective and diffusive flows, this paper presents advection-diffusion and Maxwell-Stefan models of oxygen advective flow and diffusion in response to reactions at depth. The problem is illustrated in Figure 2 and is similar to the experimental setup of *Wisotzky* [1994]. A one-dimensional soil column is connected to the atmosphere at the surface and subject to oxygen removing reactions at a reaction plane located some distance below the surface. The reaction plane is actually a moving boundary [see, e.g., *van Berk and Wisotzky*, 1995], but is considered to be immobile, an assumption that is reasonable in many cases. The model includes two components, nitrogen and oxygen. Other gases are significant in some problems [*Harries and Ritchie*, 1985; *Andersen et al.*, 2001] but are not considered here. At the bottom boundary some reaction is removing all oxygen instantaneously, or at a rate faster than the advective/diffusive processes included in the model. In experiments, the pyrite boundary is diffuse and not a sharp front as modeled here [*Elberling and Nicholson*, 1996] and while temperature driven advection can be important in many problems [*Pantelis and Ritchie*, 1991], it is not considered here. The modeled system is therefore an idealization (and not a real system) that is intended to demonstrate the relative importance of the diffusive and advective processes.

[11] Two alternate model formulations are presented and compared in this paper. The first is the advection-diffusion model favored by many hydrogeologists and the second the Maxwell-Stefan formulation favored by chemical engineers.

After presentation of the models some simple analytical solutions are presented allowing insight to be obtained into solution behavior. Following this, more general numerical solutions are presented and some overall conclusions are drawn.

## 2. Advection-Diffusion Formulation

[12] The advection-diffusion model is the most widely used by hydrogeologists and has separate advection and diffusion terms. There are many ways the equations can be presented, depending on the choice of independent variables and this choice is important when constructing a numerical solution. Here the equations are formulated in terms of the total gas pressure $p$ and the mass fraction of nitrogen $\omega_2$. The total pressure is chosen because it is expected to be well defined and changes are small throughout the domain. The nitrogen mass fraction is chosen as the second independent variable because the bottom boundary condition can be written naturally in terms of the nitrogen mass fraction. The formulation presented has two main advantages over other possibilities: the independent variables are slowly varying and the governing equations are only weakly coupled.

[13] The formulation consists of a mass balance statement for the total gas pressure $p$ [$ML^{-1}T^{-2}$] and the mass fraction of nitrogen $\omega_2$ (dimensionless), respectively [*Bird et al.*, 2002]:

$$\frac{\partial(\theta\rho)}{\partial t} - \nabla.\left(\frac{\rho\mathbf{k}}{\mu}(\nabla p - \rho\mathbf{g})\right) = 0 \tag{2}$$

$$\frac{\partial(\theta\rho\omega_2)}{\partial t} + \nabla.(\rho\omega_2\mathbf{q}) - \nabla.(\rho\mathbf{D}_2\nabla\omega_2) = 0 \tag{3}$$

where $\theta$ is the volumetric air content (dimensionless), $\rho$ is the gas density [$ML^{-3}$], $\mathbf{k}$ is the effective permeability [$L^2$], $\mu$ is the gas viscosity [$ML^{-1}T^{-1}$], $\mathbf{g}$ is the gravity vector [$LT^{-2}$] (note that the vertical coordinate is oriented positive down); and $\mathbf{q}$ is the total gas volumetric flux [$LT^{-1}$]. The nitrogen dispersion $\mathbf{D}_2$ is defined in one dimension by $D_2 = \alpha_L|v| + \tau_f D_2^m$ where $\alpha_L$ is the longitudinal dispersivity coefficient [$L^2$], $v = q/\theta$ is the gas velocity, $\tau_f = 0.66\phi\left(\frac{\theta}{\phi}\right)^2$ is the gas phase tortuosity factor (dimensionless) defined by *Moldrup et al.* [1997] in terms of the porosity $\phi$, and $D_2^m$ is the free molecular diffusion constant of nitrogen [$L^2T^{-1}$].

[14] The equation system is closed by specification of several constitutive relations, these being an equation for the molecular weight of the gas mixture, the ideal gas law, the viscosity as a function of gas composition [*Bird et al.*, 2002, equation 1.3–2c], and Darcy's law:

$$M = \left(\frac{\omega_2}{M_2} + \frac{1-\omega_2}{M_1}\right)^{-1} \tag{4}$$

$$\rho = \frac{pM}{RT} \tag{5}$$

$$\mu = \mu_1(1 - x_2) + \mu_2 x_2 \tag{6}$$

$$\mathbf{q} = -\frac{\mathbf{k}(\theta)}{\mu}(\nabla p - \rho\mathbf{g}) \tag{7}$$

where $x_2$ is the mole fraction of nitrogen given by

$$x_2 = \frac{\omega_2 M_1}{M_2 + \omega_2(M_1 - M_2)} \tag{8}$$

and where $M$ is the molecular weight of the gas mixture in terms of its component molecular weights $M_i$, $R$ is the gas constant, $T$ the temperature and $\mu$ is the gas viscosity in terms of the component viscosities $\mu_i$. Equations (4) and (8) follow from the definitions of the variables.

[15] The variables in the one-dimensional form of these equations are $p$, $\omega_2$, $\rho$, $\mu$, $M$, $q$. All other parameters are defined by the user and are constants. The boundary conditions are

$$\omega_2|_{z=0,t} = 0.768 \tag{9}$$

$$\omega_2|_{z=L,t} = 1 \tag{10}$$

$$p|_{z=0,t} = \text{atmospheric} = 1.013 \times 10^5 \ \text{Pa} \tag{11}$$

$$(\rho\omega_2 q - \rho D_2 \nabla\omega_2)|_{z=L,t} = 0 \tag{12}$$

Equations (9), (10) and (11) are direct expressions of the gas composition at the boundaries. Equation (12) states that the total nitrogen flux at the bottom boundary must be zero. This boundary condition is correct at steady state as there must be no net accumulation of nitrogen below the reaction plane. For transient simulations the boundary condition is correct if there is no gas phase below the reaction plane as there will then be no net transfer of nitrogen across the bottom boundary. The transient case with a gas phase below the reaction plane is not considered further here.

## 3. Maxwell-Stefan Formulation

[16] The advection-diffusion model of gaseous diffusion is not well suited to many gas transport problems [*Thorstenson and Pollock*, 1989; *Massmann and Farrier*, 1992; *Krishna and Wesselingh*, 1997; *Benes and Verweij*, 1999; *AbuElShar and Abriola*, 1997]. The Maxwell-Stefan formulation is less widely used in hydrological applications, but has many advantages over the advection-diffusion formulation. The Maxwell-Stefan equations are a fundamental set of equations for description of mass and heat transfer in media on a macroscopic scale. They are equivalent to the Onsager formulation from thermodynamics of irreversible processes, but have a different form. They are more general than the advection diffusion formulation because they are stated as a balance of forces and so it is relatively easy to see how to incorporate extra terms to describe processes like electrical or chemical potential gradients.

[17] The Maxwell-Stefan model is related to the dusty gas model which can be regarded as a special case of the Maxwell-Stefan equations. The dusty gas model allows

the prediction of the transport coefficients in the Maxwell-Stefan equations. The relationship between the Dusty gas model and Maxwell-Stefan equations is described by *Krishna and Wesselingh* [1997] and *Wesselingh and Krishna* [2000]. The Maxwell Stefan equations are more than a simplification of the dusty gas model: they are much more fundamental.

[18] One of the main practical differences between the Maxwell-Stefan and advection diffusion formulations is that in the advection-diffusion model of a three component system, the gas diffusion coefficients become nonlinear functions of composition [*Jaynes and Rogowski*, 1983], while in the Maxwell-Stefan formulation, the friction coefficients are constants. This means that the Maxwell-Stefan equations are easier to generalize to 3 or more component systems.

[19] For the relatively simple binary gas problem considered in this paper, the formulations are both fairly straight forward because the diffusion coefficients in the advection-diffusion model are constants. Both models are presented and compared here, and have similar results. However, the Maxwell-Stefan formulation is a better choice when more complex problems are analyzed. For example, *De Visscher and Van Cleemput* [2003] show how the Maxwell-Stefan formulation can be applied to describe a transient four component gas system.

[20] The Maxwell-Stefan equations for the 1-D problem illustrated in Figure 2 are [*Krishna and Wesselingh*, 1997; *Thorstenson and Pollock*, 1989]

$$-\frac{dp_1}{dz}+\frac{p_1M_1g}{RT}=\zeta_{12}\left(x_2N_1^D-x_1N_2^D\right)+\zeta_{1M}N_1^D \tag{13}$$

$$-\frac{dp_2}{dz}+\frac{p_2M_2g}{RT}=\zeta_{12}\left(x_1N_2^D-x_2N_1^D\right)+\zeta_{2M}N_2^D \tag{14}$$

The first term represents pressure forces, the second gravitational force. These are balanced by gas-gas friction (free diffusion) and gas solid friction (Knudsen diffusion) on the right hand side. In the above $p_1$, $p_2$ are the oxygen and nitrogen partial pressures respectively $[ML^{-1}T^{-2}]$, $\zeta_{12}=\frac{\tau^2}{\gamma}\frac{RT}{D_{12}}$ is the nitrogen/oxygen friction coefficient $[T^{-1}]$ in terms of the tortuosity $\tau$ $[-]$, the constriction factor $\gamma$ (dimensionless) [*Caron and Nkongolo*, 2004], and the free molecular diffusion coefficient $D_{12}$, $\zeta_{1M}=\frac{RT}{D_{1M}}$ is the oxygen/solid matrix friction coefficient $[T^{-1}]$ in terms of the Knudsen diffusion coefficient $D_{1M}$, $N_i^D$ are the diffusive molar fluxes of gas $i$ $[ML^{-2}T^{-1}]$, $x_i$ is the mole fraction of gas $i$ (dimensionless), $M_i$ is the molecular weight of gas $i$ $[M]$, $g$ is the acceleration due to gravity $[LT^{-2}]$, $R$ the gas constant, and $T$ is the absolute temperature.

[21] When the bulk gas is moving due to external total pressure gradients, an extra equation is needed to describe the viscous flux, this is the Darcy equation, here given as a molar flux instead of a mass flux as presented in equation (7)

$$N^v=-\frac{kp}{RT\mu}\left(\frac{dp}{dz}-\rho g\right) \tag{15}$$

where $N^v$ is the viscous molar flux [mol $L^{-2}T^{-1}$], $k$ is the permeability $[L^2]$, $p$ the total gas pressure $[ML^{-1}T^{-2}]$ and $\rho$ the total gas density $[ML^{-3}]$. A mass balance statement can be written for each of the two phases

$$\frac{\theta}{RT}\frac{\partial p_i}{\partial t}+\frac{\partial N_i}{\partial z}=0 \tag{16}$$

where

$$N_i=x_iN^v+N_i^D \tag{17}$$

is the total flux of component $i$. The system is closed by the ideal gas law (5) and a number of constitutive relationships that follow from the variable definitions:

$$p_1+p_2=p \tag{18}$$

$$x_i=\frac{p_i}{p} \tag{19}$$

$$M=x_1M_1+x_2M_2 \tag{20}$$

$$\mu=x_1\mu_1+x_2\mu_2 \tag{21}$$

The permeability can be described using the Kozeny Carmen relationship

$$k=\frac{d_m^2}{180}\frac{\epsilon^3}{(1-\epsilon)^2} \tag{22}$$

where $d_m$ is the median grain size $[L]$ and $\varepsilon$ is the porosity (dimensionless). Note that the Kozeny Carmen relationship is used to obtain a grain size that is consistent with the permeability used. This ensures comparability of the advection-diffusion and Maxwell Stefan models.

[22] The problem has unknowns $p_1$, $p_2$, $p$, $x_1$, $x_2$, $N_1$, $N_2$, $N^v$,$N_1^D$, $N_2^D$, $\mu$, $\rho$, $M$, $k$ and is solved on $z \in [0, L]$ subject to $p(0) = 1.013 \times 10^5$ Pa, $x_2(L) = 1.0$, $x_2(0) = 0.79$, $N_2(L) = 0$. These boundary conditions are equivalent to those employed for the advection-diffusion formulation (9, 10, 11, 12).

[23] Note that the Maxwell-Stefan formulation does not include dispersive mixing. In principle, dispersion could be added to the model, however this is a topic that has not been resolved in the literature and so is not addressed here.

## 4. Formulation of Maxwell-Stefan Equations for Solution

[24] For the numerical solutions, the Maxwell-Stefan equations are recast in a different form from that above. As with the advection-diffusion approach, the independent variables will be one of the component mole fractions (in this case we choose oxygen $x_1$) and the pressure $p$. To form these equations (13) and (14) can be solved for $N_i^D$ with result

$$N_1^D=-\left\{\zeta_{12}x_1\left(\frac{dp}{dz}-g\rho\right)+\zeta_{2M}\left(\frac{dp_1}{dz}-\rho_1g\right)\right\}/\zeta_e \tag{23}$$

$$N_2^D = -\left\{\zeta_{12}x_2\left(\frac{dp}{dz} - g\rho\right) + \zeta_{1M}\left(\frac{dp_2}{dz} - \rho_2 g\right)\right\}/\zeta_e \quad (24)$$

$$\zeta e = x_1\zeta_{1M}\zeta_{12} + x_2\zeta_{2M}\zeta_{12} + \zeta_{1M}\zeta_{2M} \quad (25)$$

where $\rho_i$ is the gas density of component $i$. Substituting these diffusive flux expressions with (15) into (17) results in the equations for the total gas molar fluxes

$$N_1 = -\frac{1}{\zeta e}\left[x_1\left(\frac{kp\zeta_e}{RT\mu} + \zeta_{12}\right)\left(\frac{dp}{dz} - g\rho\right) + \zeta_{2M}\left(\frac{dp_1}{dz} - \rho_1 g\right)\right] \quad (26)$$

$$N_1 = -\frac{1}{\zeta e}\left[x_2\left(\frac{kp\zeta_e}{RT\mu} + \zeta_{12}\right)\left(\frac{dp}{dz} - g\rho\right) + \zeta_{1M}\left(\frac{dp_2}{dz} - \rho_2 g\right)\right] \quad (27)$$

The first equation is the oxygen component equation. This is formed by replacing $p_1$ with $x_1p$ in (26) and then combining with (16).

$$\frac{\theta p}{RT}\frac{\partial x_1}{\partial t} + \frac{\theta}{RT}\frac{\partial p}{\partial t}x_1 - \frac{\partial}{\partial z}\left[\frac{\zeta_{2M}p}{\zeta e}\frac{\partial x_1}{\partial z}\right] - \frac{\partial}{\partial z} \cdot \left[\frac{1}{\zeta e}\left(\left(\frac{kp\zeta e}{RT\mu} + \zeta 12\right)\left(\frac{\partial p}{\partial z} - g\rho\right) + \zeta_{2M}\left(\frac{\partial p}{\partial z} - \frac{pM_1}{RT}g\right)\right)x_1\right] = 0 \quad (28)$$

An equation in pressure can be derived from the nitrogen component molar flux (27) and (16).

$$\frac{\theta x_2}{RT}\frac{\partial p}{\partial t} + \frac{\theta}{RT}\frac{\partial x_2}{\partial t}p - \frac{\partial}{\partial z}\left[\frac{x_2}{\zeta e}\left(\frac{kp\zeta e}{RT\mu} + \zeta_{12} + \zeta_{1M}\right)\frac{\partial p}{\partial z}\right] + \frac{\partial}{\partial z}\left[\left(\frac{x_2}{\zeta_e}\left(\frac{kp\zeta_e}{RT\mu} + \zeta_{12}\right)\frac{gM}{RT} + \frac{\zeta_{1M}}{\zeta_e}\left(\frac{M_2 g}{RT} - \frac{\partial x_2}{\partial z}\right)\right)p\right] = 0 \quad (29)$$

## 5. Analytical Solution of the Advection-Diffusion Model: Steady State

[25] In this section a simple one-dimensional analytical solution describing evaporation from a surface [see *Bird et al.*, 2002] is applied to the gas flow problem described in this paper. At steady state there is no net accumulation of nitrogen in the soil column, and since the net nitrogen flux is zero at the bottom of the column, it is zero throughout. This implies that at every point in the column the advective nitrogen flux is matched by an equal and opposite nitrogen diffusive flux.

$$\rho\omega_2 q - \rho D_2\frac{d\omega_2}{dz} = 0 \quad (30)$$

Solving for $q$,

$$q = \frac{D_2}{\omega_2}\frac{d\omega_2}{dz} \quad (31)$$

The gas mass balance equation (2) in one dimension and at steady state is

$$\frac{d}{dz}(\rho q) = 0 \quad (32)$$

These equations are subject to the boundary conditions

$$\omega_2|_{z=0,t} = a \quad (33)$$

$$\omega_2|_{z=L,t} = 1 \quad (34)$$

Here, the top boundary condition is written for an arbitrary atmospheric nitrogen mass fraction $a$. Substituting (31) into (32) and assuming that $\rho$ and $D_2$ are constant gives the ODE

$$\frac{d}{dz}\left(\frac{1}{\omega_2}\frac{d\omega_2}{dz}\right) = 0 \quad (35)$$

whose solution with the boundary conditions (33) and (34) is

$$\omega_2 = (a)^{\frac{L-z}{L}} \quad (36)$$

The solution is shown in Figure 3 for $a = 0.768$ (see steady state solution in Figure 3). Since $q$ is a constant and $\omega_2$ increases with depth it can be seen that the advective flux of nitrogen increases nonlinearly with depth and is balanced by an equal and opposite increasing diffusive flux. Intuitively, the curvature in the solution $\omega_2$ can be explained as a downward advection of a linear diffusion profile, giving the final profile its slight curvature.

[26] The solution can be used to calculate the advective and diffusive fluxes of oxygen at the surface. The advective flux of oxygen at the surface is given by

$$(1-\omega_2)\rho q|_{z=0} = -\frac{(1-a)\ln(a)\rho D_2}{L} \quad (37)$$

The diffusive flux of oxygen at the surface is equal in magnitude, but opposite in direction to the diffusive nitrogen flux and is given by (30) to be

$$\rho D_2\frac{\partial\omega_2}{\partial z}|_{z=0} = \omega_2\rho q|_{z=0} = -\frac{a\ln(a)\rho D_2}{L} \quad (38)$$

Both the advective and diffusive fluxes are inversely proportional to $L$ showing that oxygen transport will be fastest when the reaction plane is near the surface and concentration and pressure gradients are large. If the reactions are rate limited by oxygen transport, then the reaction rate will also be inversely proportional to $L$.

[27] The total flux is given by the sum of equations (37) and (38)

$$F = -\frac{\rho D_2\ln(a)}{L} \quad (39)$$

This equation could be used as a screening tool to estimate pyrite oxidation rates. One widely used screening tool is the Crank solution [*Crank*, 1975]

$$F = C_o\sqrt{KD_e} \quad (40)$$

where $C_o$ is the oxygen concentration at the surface, $K$ is the first-order pyrite reaction rate and $D_e$ is the effective

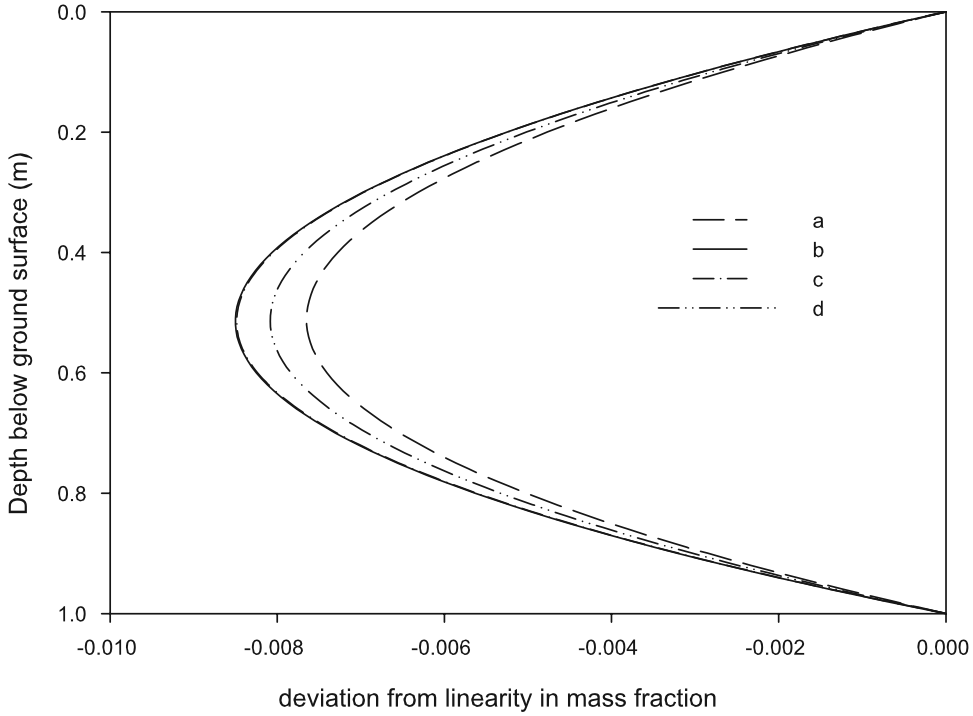


**Figure 3.** Comparison of steady state solutions to the gas flow problem. The difference between each solution and the linear profile $\omega_2 = 0.768 + (1.0 - 0.768)z$ is shown. Curve a, analytical advection-diffusion solution, constant density; curve b, analytical advection-diffusion solution, density varying with composition; curve c, numerical advection-diffusion solution; curve d, numerical solution of the Maxwell-Stefan equations.

diffusion coefficient. Both tools have value: equation (39) applies to systems which are transport limited (reaction rates are faster than transport rates), while equation (40) accounts for reaction kinetics and will apply in cases that are reaction rate limited.

[28] Equations (37) and (38) give the surprisingly simple result that at steady state the diffusive flux of oxygen at the ground surface is $\frac{a}{1-a}$ times larger than the advective flux. This ratio is independent of the length of column and soil properties and is determined entirely by the boundary conditions. As the amount of oxygen in the atmosphere increases, the advection increases in importance. In fact, the advective flux of oxygen as a portion of the total flux at the surface is simply given by $1 - a$. In the limiting system consisting of a pure oxygen atmosphere, the system is entirely driven by advection.

[29] Most authors [e.g., *Elberling and Nicholson*, 1996] have calculated oxygen mass fluxes using a simple diffusive approximation with the flux being given by

$$F_{diff} = -\rho D \frac{d\omega_1}{dz} = \frac{\rho D(1-a)}{L} \tag{41}$$

This approximation results in a linear concentration profile if the only sink of oxygen is at the bottom boundary. It is useful to consider the error made when using this approach. Given that the total flux is given by equation (39), then the error is $\frac{(1-a)+\ln(a)}{\ln(a)}$. For $a = 0.768$ the error made by using a diffusive approximation is 12.1%. As $a \rightarrow 0$ the system becomes increasingly driven by advection and the error $\rightarrow$ 100%.

[30] The analytical solution presented here is limited by the assumption of constant density and $D_2$. A more general solution can be obtained where density is allowed to vary with gas composition, while the gas pressure is assumed to be constant. It can be derived in a similar manner to the above if the equations are recast in terms of the mole fraction

$$x_2 = \omega_2 M(\omega_2)/M_2 \tag{42}$$

then equation (31) becomes

$$q = \frac{D_2 M_1}{M x_2} \frac{dx_2}{dz} \tag{43}$$

The equation solved is the nitrogen mass balance (32) which is combined with $q$ given by (43) and $\rho$ given by (5) to find (provided $p$ and $T$ are constants)

$$\frac{d}{dz}\left(\frac{1}{x_2}\frac{dx_2}{dz}\right) = 0 \tag{44}$$

subject to the boundary condition

$$x_2|_{z=0,t} = \hat{a} \tag{45}$$

The solution is

$$x_2 = (\hat{a})^{\frac{L-z}{L}} \tag{46}$$

The two analytical solutions are shown in Figure 3 together with two numerical solutions to the advection-diffusion and

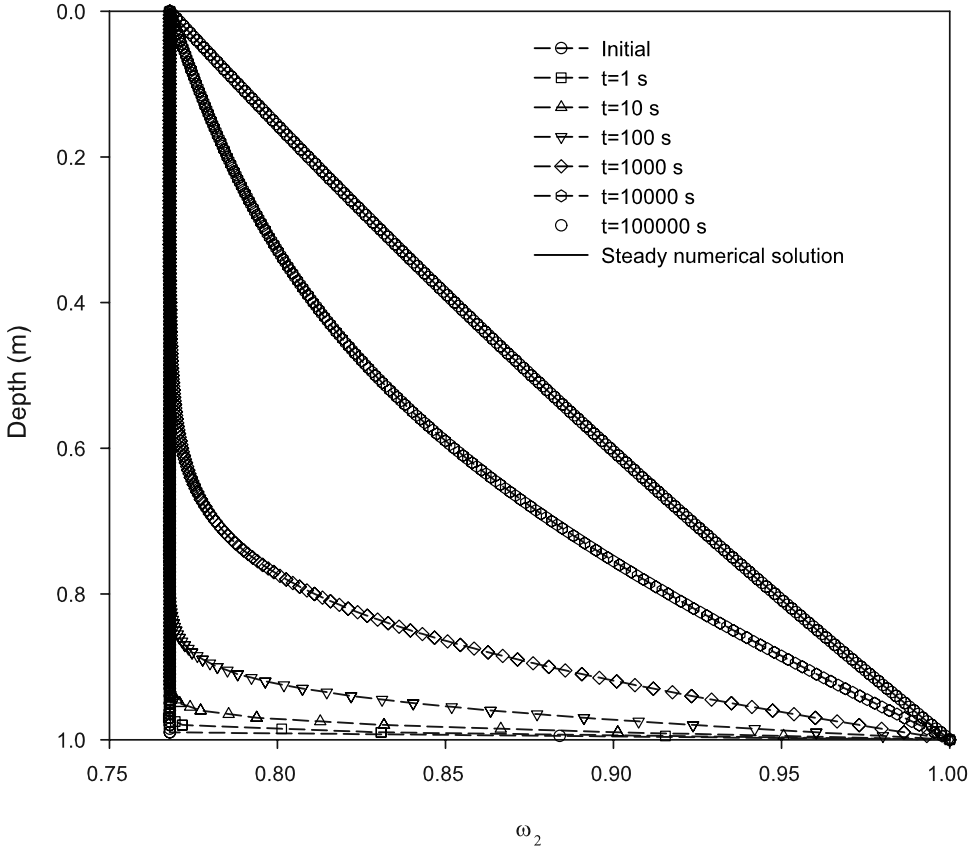


**Figure 4.** Transient simulation of nitrogen mass fraction. The 1 m column initially contains air of atmospheric composition (76.8% nitrogen, 23.2% oxygen). Reactions remove oxygen at a depth of 1 m, and the air composition changes until steady state is reached at approximately 100,000 s (~28 hours).

Maxwell-Stefan equations (see below for details). The parameters used in the analytical solutions presented in Figure 3 are $L = 1$, $M_1 = 0.032$ kg, $M_2 = 0.028$ kg and $a = 0.768$. It can be seen that the solution (46) (curve b) almost exactly describes the solution to the complete equations (curve c). The constant density solution (36) (curve a) is a good approximation of the solution and so the insights provided by it are valid.

## 6. Numerical Solutions

[31] The governing equations were solved using the generic finite element solver MULTIPHYSICS 3.2. For the advection-diffusion model, the equations solved are (2) and (3) for pressure and nitrogen mass fraction respectively, subjected to the boundary conditions (9), (10), (11) and (12). For the Maxwell-Stefan model, the equations solved are (28) and (29) for the oxygen mole fraction and pressure respectively, subject to boundary conditions that are equivalent to those employed in the advection-diffusion model. Solutions were checked against the analytical solutions and the advection-diffusion model was checked against an independently written finite element solution coded by the authors.

## 7. Results

[32] Results of the numerical models are now presented. Firstly the advection-diffusion model is used to analyses various example problems. Then a comparison is made to the Maxwell-Stefan model and some comments are made.

### 7.1. Example Calculation: Column Initially Filled With Air

[33] To illustrate the solution behavior an example is presented where a $L$ = 1m long column of soil initially containing air and dry sand is subject to oxygen removing reactions at the lower boundary. The advection-diffusion model is set up with parameters typical for sand $\theta = 0.3$, $\alpha = 0.01$ m, $D_2^m = 0.202 \times 10^{-4}$ m$^2$ s$^{-1}$, $\phi = 0.3$, $\tau_f = 0.25$, $k = 1.0 \times 10^{-11}$ m$^2$, $\mu_1 = 20.8 \times 10^{-6}$ kg m$^{-1}$ s$^{-1}$, $\mu_2 = 17.9 \times 10^{-6}$ kg m$^{-1}$ s$^{-1}$, $g = 9.81$ ms$^{-2}$, $M_1 = 0.032$ kg, $M_2 = 0.028$ kg, $R = 8.314$ J mol$^{-1}$ K$^{-1}$, and $T = 298$°K. As initial condition, the soil column is assumed to contain air with atmospheric composition, that is [*Eagleson*, 1970]

$$\omega_2|_{z,t=0} = 0.768 \tag{47}$$

$$p|_{z,t=0} = p_o \exp\left(\frac{Mgz}{RT}\right) \tag{48}$$

Results are shown in Figures 4 and 5. Figures 4 and 5 show a decelerating change from the initial condition toward the steady state. The steady state is a slightly curved profile, with the deviation from linearity due to air advection.

[34] Figure 5 shows the component advective and diffusive fluxes at the surface. The diffusive flux shown is for

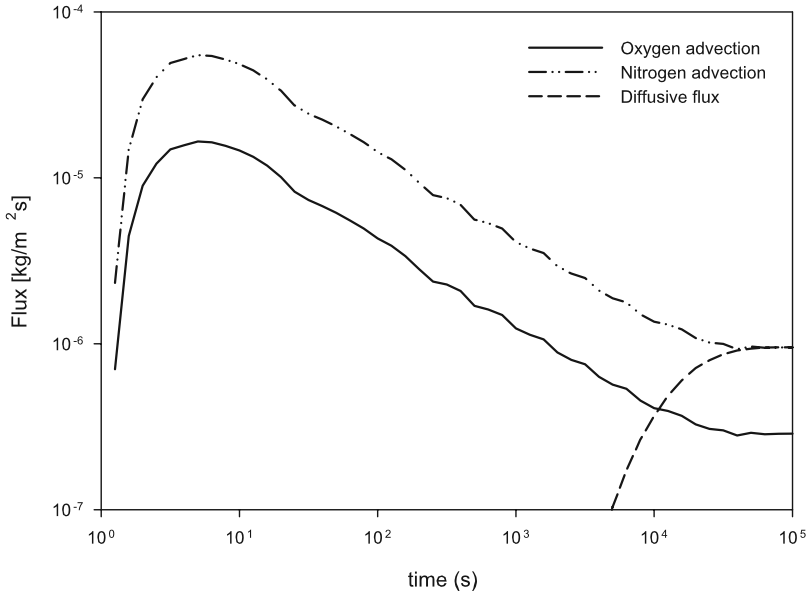


**Figure 5.** Mass fluxes of each gas at the surface.

both gases, however the oxygen diffusive flux is into the column while the nitrogen diffusive flux is out of the column. Advective fluxes are all into the column. Initially the surface flux is zero and after a short time it becomes almost entirely advective. This is because at early times there is no concentration gradient to drive diffusion at the ground surface. However 20% of the gas volume is removed at depth causing a decrease in pressure which in turn drives an advective flux from the surface. After 1 s, the pressure at the bottom of the column is 133 Pa below atmospheric pressure (see Figure 6). With time the advective flux gradually decreases, until at a time of 10,000 s the diffusive flux of oxygen becomes greater than the advective flux. The model includes both molecular diffusion and gas dispersion. At time 1 s the dispersion is of similar magnitude to the molecular diffusion. As steady state is approached the advective flux and dispersion terms both decrease. At steady state the molecular diffusion term is about 100 times greater than the dispersion term. The extra dispersion at early times increases the rate at which the profile approaches steady state.

[35] At steady state the nitrogen diffusive flux is equal and opposite to its advective flux. The oxygen diffusive flux into the soil is 3.09 times greater than the advective flux, a result that is similar to the constant density analytical solution where the ratio was $\frac{a}{1-a} = 3.31$. At steady state, the pressure at the bottom of the column driving the advective flux is only 2.1 Pa lower than atmospheric pressure.

[36] A sensitivity analysis of the numerical advection-diffusion model shows that the model is quite insensitive to the physical parameters at steady state. The numerically computed steady state ratio between surface advective and diffusive fluxes does not depend at all on permeability and depends only slightly on column length. This result is

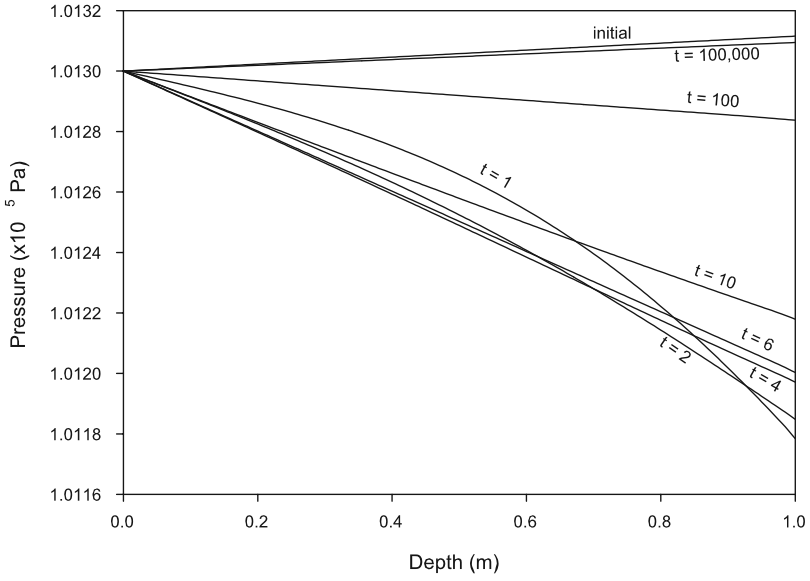


**Figure 6.** Transient pressure profiles for the simulations shown in Figure 4.

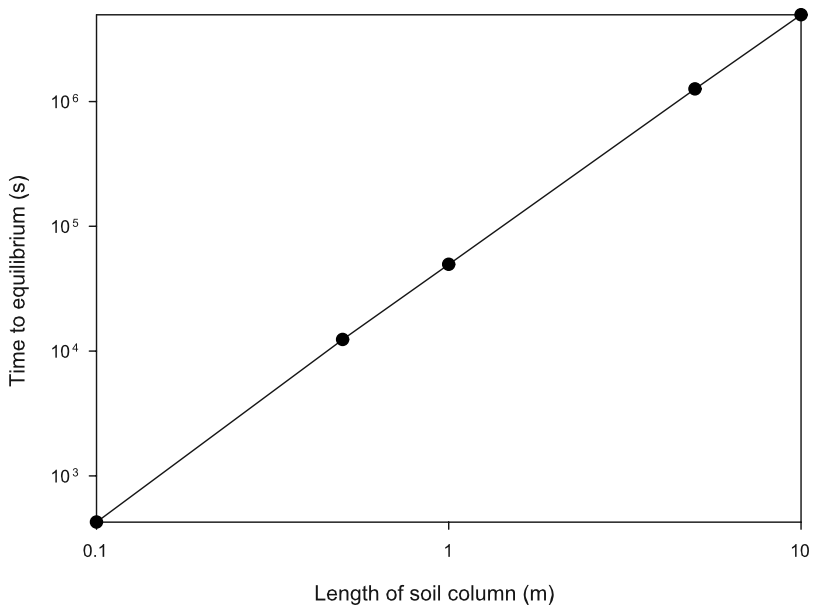


**Figure 7.** Time to reach equilibrium (0.1% of the steady state $\omega_2$ in middle of column) for various column lengths.

consistent with the analytical solution where the ratio of advective and diffusive fluxes is also independent of the physical parameters. While the surface gas flux is not sensitive to the soil permeability, the pressure deficit at the bottom of the column does depend on permeability, with a less permeable soil requiring larger pressure deficits to drive the same gas flow. As the soil becomes less permeable, the problem also becomes more challenging numerically as the pressure deviates more from hydrostatic and the system becomes more nonlinear and coupled.

[37] The steady state ratio of fluxes is almost entirely determined by the atmospheric composition. However, the transient problem is dependent on other model parameters. For example, Figure 7 shows the time required to reach equilibrium for various column lengths. It can be seen that the time to equilibrium increases exponentially with increasing column length. Curiously, while the time to equilibrium is very sensitive to column length, the time to equilibrium is relatively insensitive to permeability. A three order of magnitude decrease in permeability resulted in only a 2% increase in time to equilibrium. This paper has assumed a stationary reaction zone. Figure 7 shows that such an assumption is reasonable for short column lengths. However, as the reactive zone moves deeper below the surface, longer times are required before equilibrium is reached and over these timescales movement of the reactive zone can become significant. In these cases, the problem becomes a moving boundary problem.

### 7.2. Example Calculation: Column Initially Filled With Nitrogen

[38] *Wisotzky* [1994] reported the results of some column experiments where a column initially containing little oxygen, was opened at one end and oxygen from the atmosphere allowed to enter, and oxygen concentrations monitored as pyrite oxidation progressed (see Figure 1). A direct comparison between the model and experimental results is not possible because some features of the experiment are not included in the model. For example, in Wisotzky's experiment small amounts of pyrite were initially distributed throughout the column whereas the model assumes a sharp reaction plane. The experimental results also indicate that kinetics play a role, because oxygen is present at locations below the uppermost locations where there is pyrite. Other experimental results, for example, those of *Elberling and Nicholson* [1996], suggest that the sharp reaction plane is a valid first approximation to the problem and that approach has been taken in this work.

[39] While direct comparison with the experiments is not reasonable, it is interesting to compare model results for an initial state of a nitrogen filled column with the air filled column of the previous section. Results are shown in Figure 8. In the nitrogen filled column, advective fluxes are much less important, here the model predicts an insignificant initial pressure drop at the bottom of the column. Unlike the previous example, this problem is diffusion dominated with an initial ($t$ = 1 s) oxygen diffusive flux at the ground surface of $9.88 \times 10^{-5}$ kg/m$^2$s and advective flux of $2.86 \times 10^{-6}$ kg/m$^2$s. As steady state is approached the fluxes converge to those shown at late times in Figure 5. The reason advective fluxes are small in the nitrogen filled column experiments is that the large volume losses initially experienced in the air filled column do not occur in the $N_2$ filled column. Instead, the main fluxes are diffusion of oxygen into the column and an equal and opposite nitrogen diffusion out of the column.

### 7.3. Numerical Results: Maxwell Stefan Model

[40] The steady state Maxwell-Stefan solution is shown in Figure 3 (curve d) for parameters $M_1$ = 0.032 kg, $M_2$ = 0.028 kg, $R$ = 8.314 Jmol$^{-1}$ K$^{-1}$, $T$ = 298 K, $p_0 = 1.013 \times 10^5$ Pa, $L$ = 1.0 m, spherical porous material diameter $d = 1.6 \times 10^{-4}$ m, porosity $\varepsilon$ = 0.25, free gas diffusion constant $D_{12} = 2 \times 10^{-5}$ m$^2$ s$^{-1}$, $\zeta_{12}^0 = \frac{RT}{D_{12}}$, tortuosity $\tau$ = 1.4, constriction factor $\gamma$ = 0.7, friction coefficient $\zeta_{12} = \zeta_{12}^0 \frac{\tau^2}{\gamma}$, Knudsen diffusion coefficient $D_{1M} = d\frac{\epsilon^{1.5}}{1-\epsilon}\sqrt{\frac{8}{9\pi}\frac{RT}{M_1}}$, oxygen

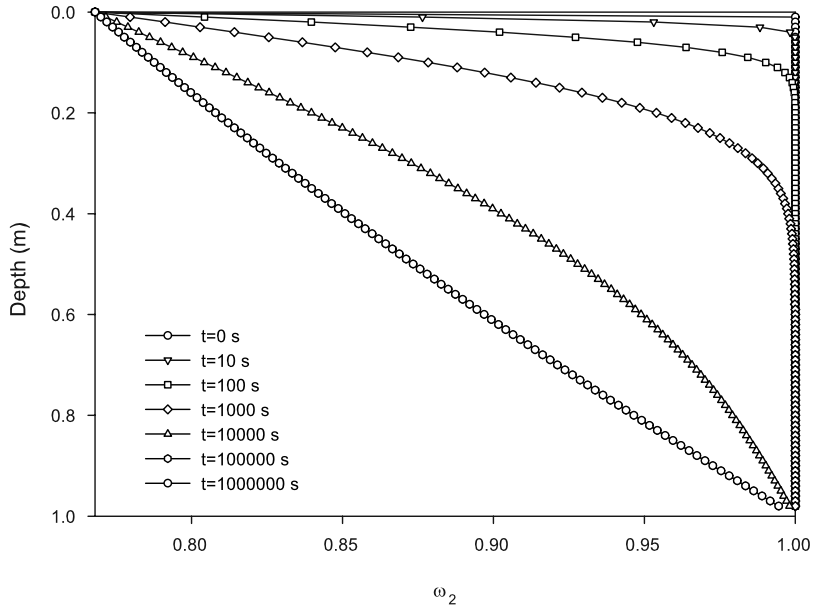


**Figure 8.** Time evolution of nitrogen mass fraction in a column initially filled with nitrogen.

matrix friction coefficient $\zeta_{1M} = \frac{RT}{D_{1M}}$. These properties can be shown using the Kozeny Carmen relationship [*Krishna and Wesselingh*, 1997] to be similar to those used in the advection-diffusion model. Figure 3 shows that advection-diffusion and Maxwell-Stefan models have similar solutions. The small difference between the two models can be attributed to differences in the way matrix friction is determined in the models and the lack of a dispersion term in the Maxwell-Stefan model. Similar good correspondence between the advection-diffusion and Maxwell-Stefan models is also obtained for the transient examples presented above.

[41] The good correspondence between the advection-diffusion and Maxwell-Stefan approaches for binary systems has been noted by others, for example, *Fen and Abriola* [2004], and our results concur with theirs. However, it should be expected that the correspondence will be poorer if more than three gas components are present. For example, *Baehr and Bruell* [1990] have shown that the advection-diffusion model gives poor results for transport of an organic component in air. The addition of a third component is straight forward in the Maxwell-Stefan formulation and this formulation should be chosen whenever there are more than two components in the gas phase.

## 8. Conclusions

[42] The simple examples considered in this paper have illustrated the importance of considering gas phase advection in reactive flow problems in unsaturated porous media. Even at steady state, gas advection is 23% of the total flux of oxygen at the surface in a column subject to typical atmospheric conditions. For a mine dump this means that current modeling approaches underestimate the rate of pyrite oxidation by 12% for air with an atmospheric composition. The error made by employing a diffusive approximation increases as the air becomes more oxygen rich.

[43] In transient simulations, large pressure deficits can be experienced at the location of reactions which drive advective fluxes that dominate gas fluxes until steady state is almost reached. The steady state fluxes are almost entirely determined by atmospheric composition. In transient cases, other parameters become significant, for example the time required to reach steady state depends exponentially on column length.

[44] Other researchers have compared experimental observations of oxygen fluxes with calculated diffusive fluxes and concluded that diffusion is the predominant oxygen transport mechanism [e.g., *Elberling and Nicholson*, 1996]. Here two formulations of gas transport have shown that advective fluxes should not be neglected in reactive gas problems. These results concur with the previous modeling studies of *Thorstenson and Pollock* [1989] and with recent experimental observations [e.g., *Wisotzky*, 1994; *Amos et al.*, 2005]. Our work reinforces the conclusions of previous studies and provide simple analytical approaches that provide insight into the system behavior.

[45] The transient simulations presented in this work are somewhat limited. They were inspired by laboratory-scale experimental systems operating on short timescales. However, the results may not apply to field problems where other processes may dominate. For these problems, additional analysis is required to include a broader range of processes over much longer timescales. Extensions might include incorporation of reactions and their kinetics, growth of microorganisms catalyzing the oxidation, the moving boundary, etc, into the model. Other gas components could be considered, for example $CO_2$ is known to comprise up to 20% of gas volume in mine waste [*van Berk and Wisotzky*, 1995]. The water phase with a variable moisture content could be explicitly included, for instance, it would be particularly interesting to examine how infiltration events affect rates of oxygen transport and subsequent pyrite oxidation. Other driving forces for gas advection such as temperature driven advection [*Pantelis and Ritchie*, 1991; *Lefebvre et al.*, 2001] and atmospheric pumping [e.g., *Elberling et al.*, 1998] are important in some problems. Finally, this paper has been written with pyrite oxidation in mind, but other geochemical processes involving gases may

involve volume changes and could be approached in a similar way.

[46] **Acknowledgments.** This research was started during the sabbatical leave of Thomas Russell and Dieke Postma at the University of Newcastle, Australia, the former employer of the first author. The support of the University of Newcastle is gratefully acknowledged. The authors have had some useful and vigorous discussion about this problem with Helge Dahle, Michael A. Celia, and others. Their interest in the work has been of great benefit. The research of the third author was supported in part by National Science Foundation grants DMS-0084438 and DMS-0222300. We would also like to acknowledge the reviewers, whose comments were useful in improving the manuscript. This paper is based on the work by *Binning et al.* [2004].

## References

AbuElShar, W., and L. M. Abriola (1997), Experimental assessment of gas transport mechanisms in natural porous media: Parameter evaluation, *Water Resour. Res.*, *33*, 505–516.

Amos, R. T., K. U. Mayer, B. A. Bekins, G. N. Delin, and R. L. Williams (2005), Use of dissolved and vapor-phase gases to investigate methanogenic degradation of petroleum hydrocarbon contamination in the subsurface, *Water Resour. Res.*, *41*, W02001, doi:10.1029/2004WR003433.

Andersen, M. S., F. Larsen, and D. Postma (2001), Pyrite oxidation in unsaturated aquifer sediments: Reaction stochiometry and rate of oxidation, *Environ. Sci. Technol.*, *35*, 4074–4079.

Baehr, A. L., and C. J. Bruell (1990), Application of the Stefan-Maxwell equations to determine limitations of Fick's law when modeling organic vapor transport in sand columns, *Water Resour. Res.*, *26*, 1155–1163.

Benes, N., and H. Verweij (1999), Comparison of macro- and microscopic theories describing multicomponent mass transport in microporous media, *Langmuir*, *15*, 8292–8299.

Binning, P., D. Postma, and T. F. Russell (2004), The balance between advection and diffusion in reactive gas transport during pyrite oxidation in the unsaturated zone, in *Computational Methods in Water Resources, Proceedings of the XVth International Conference on Computational Methods in Water Resources (CMWR XV), Chapel Hill, North Carolina, USA, June 13–17 2004*, edited by C. T. Miller et al., pp. 891–902, Elsevier, New York.

Bird, R. B., W. E. Stewart, and E. N. Lightfoot (2002), *Transport Phenomena*, 2nd ed., John Wiley, Hoboken, N. J.

Bronswijk, J., K. Nugroho, J. Aribawa, J. Groenberg, and C. Ritsma (1993), Modelling oxygen transport and pyrite oxidation in acid sulphate soils, *J. Environ. Qual.*, *22*, 544–554.

Caron, J., and N. V. Nkongolo (2004), Assessing gas diffusion coefficients in growing media from in situ water flow and storage measurements, *Vadose Zone J.*, *3*, 300–311.

Cathles, L. M., and J. A. Apps (1975), A model of the dump leaching process that incorporates oxygen balance, heat balance and air convection, *Metall. Trans. B*, *6*, 617–624.

Costanza-Robinson, M. S., and M. L. Brusseau (2002), Gas phase advection and dispersion in unsaturated porous media, *Water Resour. Res.*, *38*(4), 1036, doi:10.1029/2001WR000895.

Crank, J. (1975), *The Mathematics of Diffusion*, 2nd ed., Clarendon, Oxford, U. K.

Davis, G., and A. Ritchie (1986), A model of oxidation in pyritic mine wastes: part 1. Equation and approximate solution, *Appl. Math. Modell.*, *10*, 314–332.

De Visscher, A., and O. Van Cleemput (2003), Simulation model for gas diffusion and methane oxidation in landfill cover soils, *Waste Manage.*, *23*, 581–591.

Eagleson, P. S. (1970), *Dynamic Hydrology*, McGraw-Hill, New York.

Elberling, B., and R. V. Nicholson (1996), Field determination of sulphide oxidation rates in mine tailings, *Water Resour. Res.*, *32*, 1773–1784.

Elberling, B., F. Larsen, S. Christensen, and D. Postma (1998), Gas transport in a confined unsaturated zone during atmospheric pressure cycles, *Water Resour. Res.*, *34*, 2855–2862.

Fen, C. S., and L. M. Abriola (2004), A comparison of mathematical model formulations for organic vapor transport in porous media, *Adv. Water Res.*, *27*, 1005–1016.

Gerke, H. H., J. W. Molson, and E. O. Frind (2001), Modelling the impact of physical and chemical heterogeneity on solute leaching in pyritic overburden mine spoils, *Ecol. Eng.*, *17*, 91–101.

Harries, J. R., and A. I. M. Ritchie (1985), Pore gas composition in waste rock dumps undergoing pyritic oxidation, *Soil Sci.*, *140*, 143–152.

Jaynes, D. B., and A. S. Rogowski (1983), Applicability of Ficks law to gas-diffusion, *Soil Sci. Soc. Am. J.*, *47*, 425–430.

Kim, H., and C. H. Benson (2004), Contributions of advective and diffusive oxygen transport through multilayer composite caps over mine waste, *J. Contam. Hydrol.*, *71*, 193–218.

Krishna, R., and J. A. Wesselingh (1997), The Maxwell-Stefan approach to mass transfer, *Chem. Eng. Sci.*, *52*, 861–911.

Kuo, E. Y., and A. I. M. Ritchie (1999), The impact of convection on the overall oxidation rate in sulfidic waste rock dumps, in *Proceedings of Sudbury '99: Mining and the Environment II*, vol. 1, edited by D. Goldsacket al., pp. 211–220, Cent. in Min. and Miner. Explor. Res., Laurentian Univ., Sudbury, Ont., Canada.

Larsen, F., and D. Postma (1997), Nickel mobilization in a groundwater well field: Release by pyrite oxidation and desorption from manganese oxides, *Environ. Sci. Technol.*, *31*, 2589–2595.

Lefebvre, R., D. Hockley, J. Smolensky, and A. Lamontagne (2001), Multiphase transfer processes in waste rock piles producing acid mine drainage: 2. Applications of numerical simulation, *J. Contam. Hydrol.*, *52*, 165–186.

Massmann, J., and D. F. Farrier (1992), Effects of atmospheric pressures on gas-transport in the vadose zone, *Water Resour. Res.*, *28*, 777–791.

Mayer, K. U., E. O. Frind, and D. W. Blowes (2002), Multicomponent reactive transport modeling in variably saturated porous media using a generalized formulation for kinetically controlled reactions, *Water Resour. Res.*, *38*(9), 1174, doi:10.1029/2001WR000862.

Moldrup, P., T. Olesen, D. E. Rolston, and T. Yamaguchi (1997), Modeling diffusion and reaction in soils, VII, Predicting gas and ion diffusivity in undisturbed and sieved soils, *Soil Sci.*, *162*, 632–640.

Molson, J. W., O. Fala, M. Aubertin, and B. Bussiere (2005), Numerical simulations of pyrite oxidation and acid mine drainage in unsaturated waste rock piles, *J. Contam. Hydrol.*, *78*, 343–371.

Nordstrom, D. K., C. N. Alpers, C. J. Ptacek, and D. W. Blowes (2000), Negative pH and extreme acidic mine waters from iron mountain california, *Environ. Sci. Technol.*, *34*, 254–258.

Pantelis, G., and A. I. M. Ritchie (1991), Macroscopic transport mechanisms as rate-limiting factor in dump leaching of pyritic ores, *Appl. Math. Modell.*, *15*, 136–143.

Pantelis, G., A. I. M. Ritchie, and Y. A. Stepanyants (2002), A conceptual model for the description of oxidation and transport processes in sulphidic waste rock dumps, *Appl. Math. Modell.*, *26*, 751–770.

Simunek, J., and D. L. Suarez (1993), Modeling of carbon-dioxide transport and production in soil: 1. Model development, *Water Resour. Res.*, *29*, 487–497.

Sleep, B. E., and J. F. Sykes (1989), Modeling the transport of volatile organics in variably saturated media, *Water Resour. Res.*, *25*, 81–92.

Thorstenson, D. C., and D. W. Pollock (1989), Gas transport in the unsaturated zones: Multicomponent systems and the adequacy of Ficks laws, *Water Resour. Res.*, *25*, 477–507.

van Berk, W., and F. Wisotzky (1995), Sulphide oxidation in brown coal overburden and chemical modeling of reactions in aquifers influenced by sulphide oxidation, *Environ. Geol.*, *26*, 192–196.

Wesselingh, J. A., and R. Krishna (2000), *Mass Transfer in Multicomponent Mixtures*, Delft Univ. Press, Delft, Netherlands.

Wisotzky, F. (1994), Untersuchungen zur Pyritoxidation in Sedimenten des Rheinischen Braunkohlenreviers und deren Auswirkungen auf die Chemie des Grundwassers, *Besonders Mitt. Z. Dtsch. Gewaesserkundl. Jahrb.*, *58*, 153.

Wunderly, M. D., D. W. Blowes, E. O. Frind, and C. J. Ptacek (1996), Sulfide mineral oxidation and subsequent reactive transport of oxidation products in mine tailings impoundments: A numerical model, *Water Resour. Res.*, *32*, 3173–3187.

Xu, T. F., and K. Pruess (2001), Modeling multiphase non-isothermal fluid flow and reactive geochemical transport in variably saturated fractured rocks: 1. Methodology, *Am. J. Sci.*, *301*, 16–33.

Xu, T. F., S. P. White, K. Pruess, and G. H. Brimhall (2000), Modeling of pyrite oxidation in saturated and unsaturated subsurface flow systems, *Transp. Porous Media*, *39*, 25–56.

P. J. Binning, P. F. Boulin, and D. Postma, Institute of Environment and Resources, Technical University of Denmark, DK-2800 Lyngby, Denmark. (pjb@er.dtu.dk)

T. F. Russell, Division of Mathematical Sciences, National Science Foundation, 4201 Wilson Boulevard, Room 1025, Arlington,VA 22230, USA.

J. A. Wesselingh, Department of Chemical Engineering, University of Groningen, Postbus 7500, NL-9700 AE, Groningen, Netherlands.